ELSEVIER

Journal of Biomechanics 40 (2007) 2335–2340

JOURNAL OF BIOMECHANICS

www.elsevier.com/locate/jbiomech
www.JBiomech.com

Short communication

Modeling of biodynamic responses distributed at the fingers and the palm of the human hand–arm system

Ren G. Dong[a,*], Jennie H. Dong[b], John Z. Wu[a], Subhash Rakheja[b]

[a]*Engineering and Control Technology Branch, National Institute for Occupational Safety and Health, 1095 Willowdale Road, Morgantown, WV 26505, USA*
[b]*Department of Mechanical Engineering, Concordia University, 1455 de Maisoneuve Boulevard, W. Montreal, Canada H3G 1M8*

Accepted 11 October 2006

Abstract

The objective of this study is to develop analytical models for simulating driving-point biodynamic responses distributed at the fingers and palm of the hand under vibration along the forearm direction (z_h-axis). Two different clamp-like model structures are formulated to analyze the distributed responses at the fingers–handle and palm–handle interfaces, as opposed to the single driving point invariably considered in the reported models. The parameters of the proposed four- and five degrees-of-freedom models are identified through minimization of an rms error function of the model and measured responses under different hand actions, namely, fingers pull, push only, grip only, and combined push and grip. The results show that the responses predicted from both models agree reasonably well with the measured data in terms of distributed as well total impedance magnitude and phase. The variations in the identified model parameters under different hand actions are further discussed in view of the biological system behavior. The proposed models are considered to serve as useful tools for design and assessment of vibration isolation methods, and for developing a hand–arm simulator for vibration analysis of power tools.
Published by Elsevier Ltd.

Keywords: Hand; Finger; Hand–arm vibration; Hand-transmitted vibration; Biodynamic response

1. Introduction

Biodynamics of the hand–arm system is one of the important foundations for understanding mechanisms of vibration-induced disorders and for developing better standards for assessing risk of vibration exposure (Griffin, 1994; Dong et al., 2001). Knowledge of the biodynamic responses is also required for designing and assessing vibration isolation methods, and developing hand–arm simulators for analysis and test of powered hand tools. Many analytical models have been developed, in which a single-point hand–handle coupling is invariably considered. Such models thus do not permit for analyses of biodynamic responses distributed at the fingers and the palm of the hand. It is also difficult to relate the parameters of the reported models to the anthropometry and dynamic properties of the hand–arm system. This study thus aims at development of new models for analyses of distributed biodynamic responses of the system exposed to vibration along the z_h-axis (ISO-8727, 1997).

2. Methods

The hand–arm system griping and pushing a tool handle is represented by a clamp-like mechanical structure, which is applied to derive two different biodynamic models. In the first model (Fig. 1), the hand is virtually divided into two parts: fingers and the palm–wrist–arm structure, resulting in a four degrees-of-freedom (DOF) dynamic system. The fingers positioned on the half of the handle are represented by two effective masses M_4 and M_2 coupled through linear stiffness k_4 and viscous damping c_4. Similarly, the palm–wrist–arm structure is represented by two masses M_3 and M_1 coupled through k_3 and c_3. Two additional pairs of linear spring–damping elements couple the masses M_2 and M_1, and M_1 to the body (considered as a fixed support). The second one (Fig. 2) is a 5-DOF model. It is similar to the first model, except for the additional elements M_0, k_0, and c_0 representing the upper arm–shoulder structure.

The equations of motion for the models are used to compute dynamic forces developed at the fingers and palm, $F_{Fingers}$ and F_{Palm}, respectively, due to displacement y of the handle. The driving-point biodynamic

*Corresponding author. Tel.: +1 304 285 6332; fax: +1 304 285 6265.
E-mail address: rkd6@cdc.gov (R.G. Dong).

0021-9290/$ - see front matter Published by Elsevier Ltd.
doi:10.1016/j.jbiomech.2006.10.031

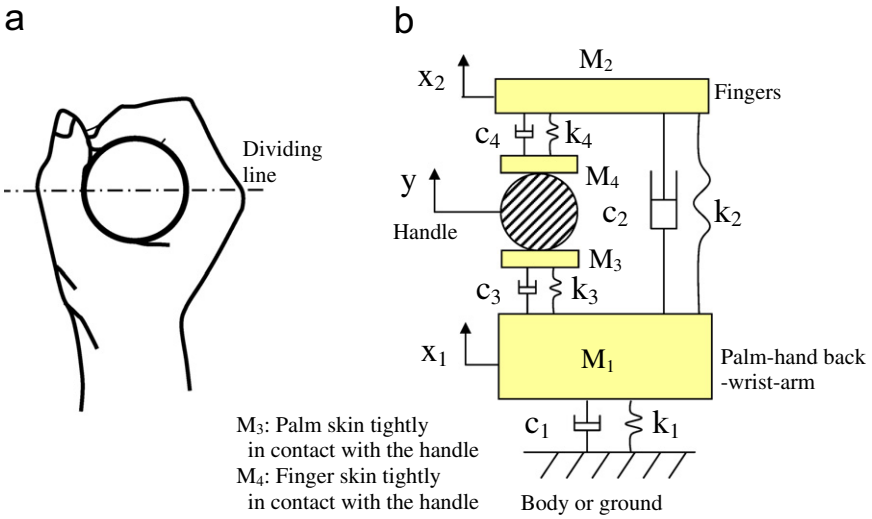

Fig. 1. Hand grip posture and a 4-DOF model representation of the fingers–hand–arm system. (a) A hand grip on a cylindrical handle and (b) A 4-DOF model.

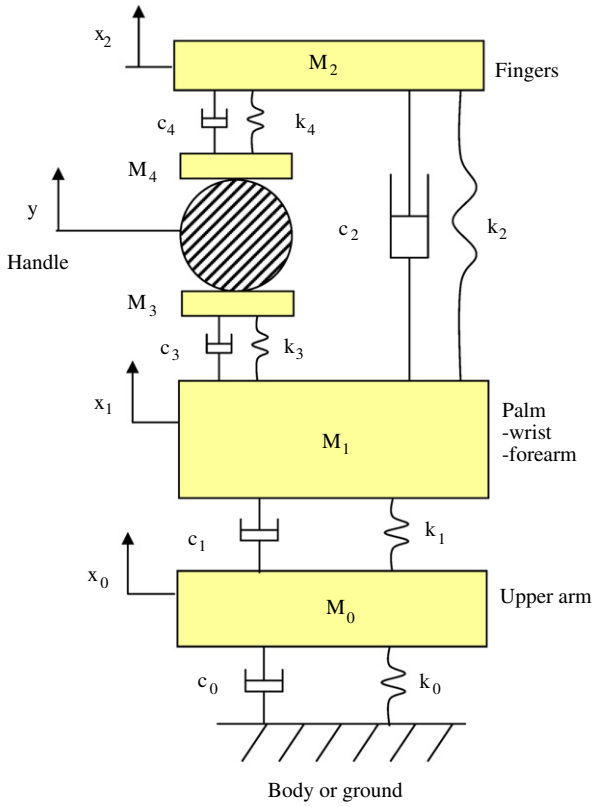

Fig. 2. A 5-DOF model representation of the fingers–hand–arm system.

responses (DPBRs) are characterized in terms of mechanical impedance (MI) at the fingers and palm–handle interfaces. Assuming excitation of the form, $y = Ye^{j\omega t}$, the distributed impedance responses (Z_{Fingers} and Z_{Palm}) are derived from

$$Z_{\text{Fingers}}(j\omega) = \frac{F_{\text{Fingers}}(j\omega)}{V(j\omega)} = \frac{(k_4 + j\omega c_4)(Y - X_2)}{j\omega Y} + j\omega M_4, \quad (1)$$

$$Z_{\text{Palm}}(j\omega) = \frac{F_{\text{Palm}}(j\omega)}{V(j\omega)} = \frac{(k_3 + j\omega c_3)(Y - X_1)}{j\omega Y} + j\omega M_3, \quad (2)$$

where $V = j\omega Y$ is the handle velocity corresponding to excitation frequency ω, and X_1 and X_2 are the magnitudes of displacement responses of M_1 and M_2, respectively. The MI of the entire hand–arm (Z_{Hand}) is computed from

$$Z_{\text{Hand}} = \frac{F_{\text{Hand}}}{V} = \frac{F_{\text{Fingers}} + F_{\text{Palm}}}{V} = Z_{\text{Fingers}} + Z_{\text{Palm}}. \quad (3)$$

The measured responses distributed at the fingers and palm have thus far been reported in a single study (Dong et al., 2005a), which was conducted with six subjects and four different hand actions (grip only, combined grip and push, push only, and pull only) using the arm posture specified in ISO10819 (1996). They were measured using a 40 mm split instrumented handle under vibration at ten discrete frequencies in the 16 to 1000 Hz range. They were used for identifying parameters of the proposed models by minimizing the rms deviations Δ between the predicted MI and the experimental data, termed as the error function $E(\chi)$:

$$E(\chi) = \text{Re}[\Delta Z_{\text{Fingers}}(j\omega)] + \text{Im}[\Delta Z_{\text{Fingers}}(j\omega)] + \text{Re}[\Delta Z_{\text{palm}}(j\omega)] + \text{Im}[\Delta Z_{\text{palm}}(j\omega)], \quad (4)$$

where 'Re' and 'Im' designate the real and imaginary components of impedance, respectively; $\Delta Z_{\text{Fingers}}$ and ΔZ_{Palm} are the deviations between the predicted and measured MI distributed at the fingers and palm, respectively, corresponding to excitation frequency ω; and χ is the vector of design parameters of each model (Figs. 1 and 2).

The parameter identification process was performed with the following constrains: $M_i \geqslant 0$; $k_i \geqslant 0$; $c_i \geqslant 0$; and $M_0 < 10$ kg. An iterative algorithm was developed to minimize $E(\chi)$ by varying each parameter in a sequential manner, while the others were held to their last updated values. An iteration cycle was completed when all the parameters were updated, and convergence was considered when difference between the error magnitudes in two consecutive cycles approached less than 0.01N s/m. The identification process was repeated by considering more than five different initial vectors. All the trials converged to similar solutions suggesting uniqueness of the solution.

3. Results

Table 1 lists the parameters identified for the 4-DOF model for the four hand actions, together with its natural frequencies. Figs. 3–6 illustrate comparisons of predicted magnitude and phase responses (Z_{Fingers}, Z_{Palm} and Z_{Hand}) of the model with the corresponding measured data. The

Table 1
Parameters for the 4-DOF model

Parameter	Unit	Hand coupling condition (50 N applied in each action)			
		Grip	Grip + push	Push	Pull
M_1	kg	1.4329	1.4145	1.1043	0.9337
M_2	kg	0.0897	0.0820	0.3110	0.0957
M_3	kg	0.0230	0.0267	0.0246	0
M_4	kg	0.0147	0.0140	0	0.0143
K_1	N/m	3377	4207	953	102
K_2	N/m	12,710	6523	1569	23,934
K_3	N/m	29,906	58,555	43,177	0
K_4	N/m	190,041	207,964	1760	187,458
C_1	N s/m	50.6	85.9	74.3	69.9
C_2	N s/m	35.2	37.9	2.0	44.1
C_3	N s/m	74.5	118.3	99.3	0
C_4	N s/m	127.6	120.8	4.2	110.5
$^*f_1$	Hz	28	35	16	24
$^*f_2$	Hz	239	257	32	237

$^*f_1$ and f_2 are undamped natural frequencies of the model.

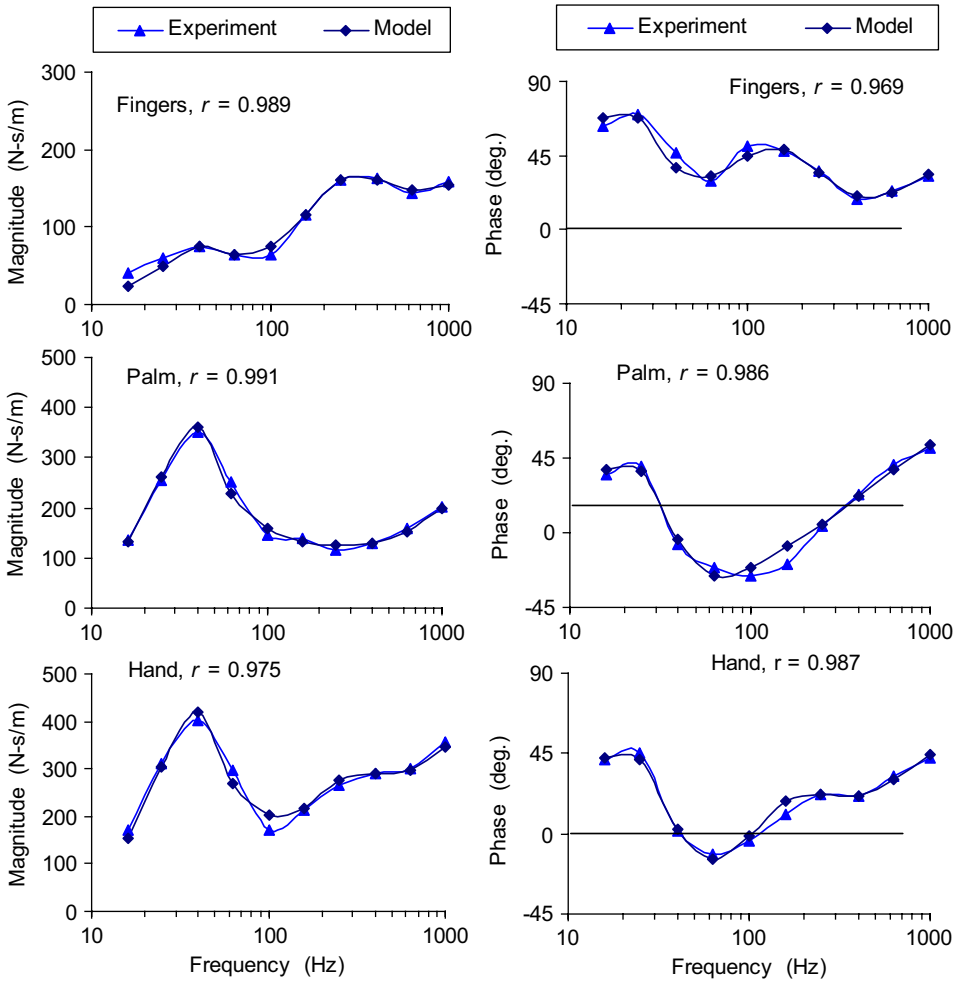

Fig. 3. Comparisons of model results with the experimental data in terms of mechanical impedance components distributed at the fingers and the palm of the hand for the combined action of 50 N grip and 50 N push.

correlation coefficient r-value between each pair of data, used to judge goodness of the curve fit, is also shown in figures. The r-value is 0.969 in the worst case.

Table 2 summarizes parameters identified for the 5-DOF model. With the exception of M_0, k_0, c_0, k_1, c_1, and f_0, they are comparable with those of the 4-DOF model. The

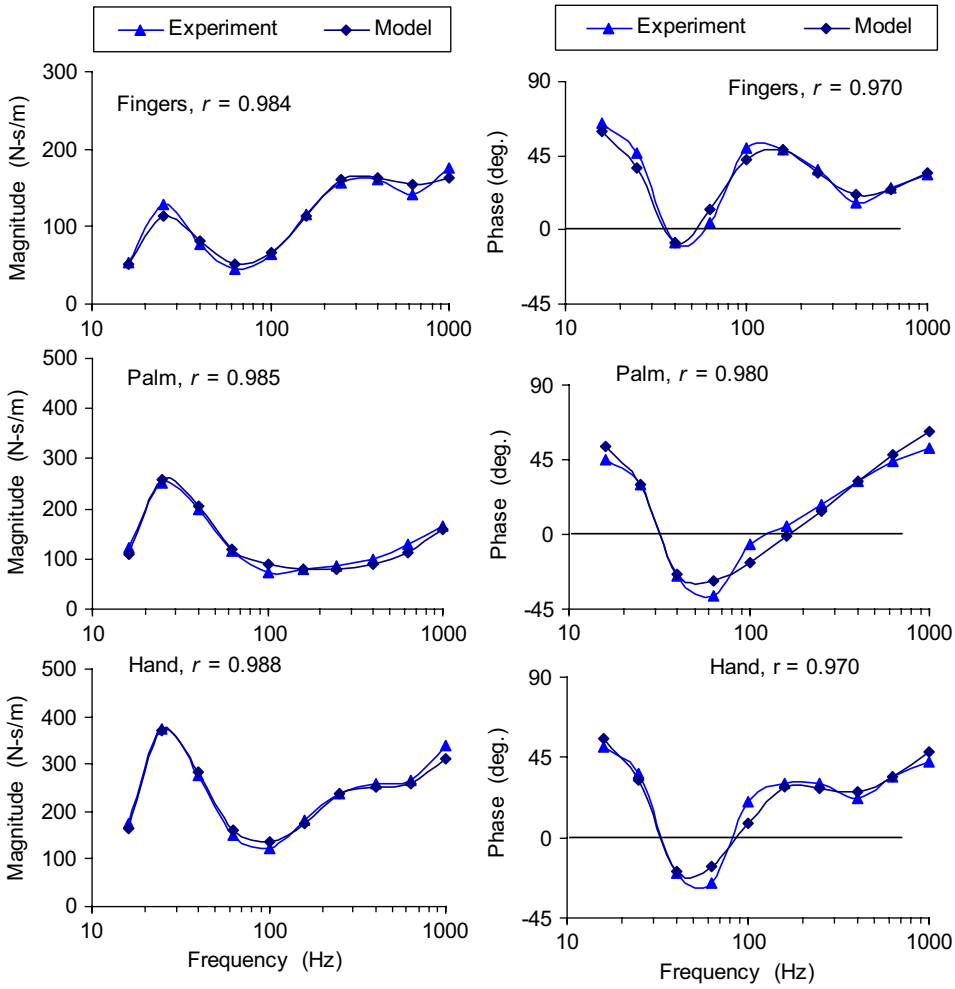

Fig. 4. Comparisons of model results with the experimental data in terms of mechanical impedance components distributed at the fingers and the palm of the hand for the 50 N grip-only action.

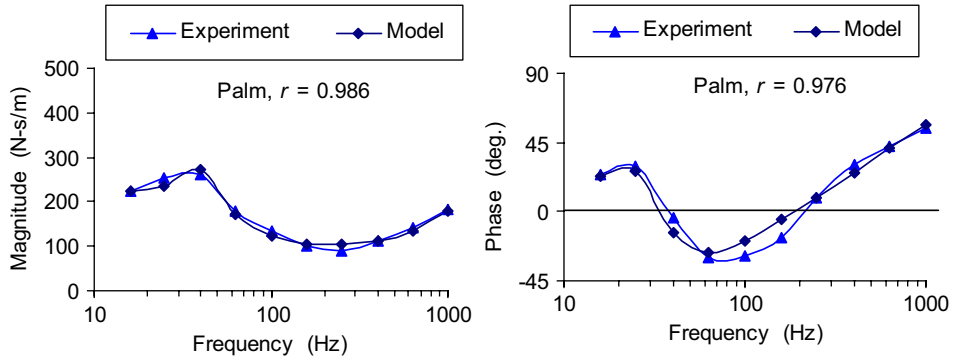

Fig. 5. Comparisons of model results with the experimental data in terms of mechanical impedance distributed at the palm of the hand for the 50 N push-only action.

magnitude of the rms errors in magnitude and phase attained for the 4- and 5-DOF models are compared in Table 3. Results suggest that the 5-DOF model generally yields errors that are slightly lower than the 4-DOF model.

4. Discussion and conclusions

The uncoupled natural frequency of the finger mass, estimated from $\sqrt{k_4/M_2}$, for each of the three actions (grip: 232 Hz; grip + push: 253 Hz; and pull: 223 Hz) is close to

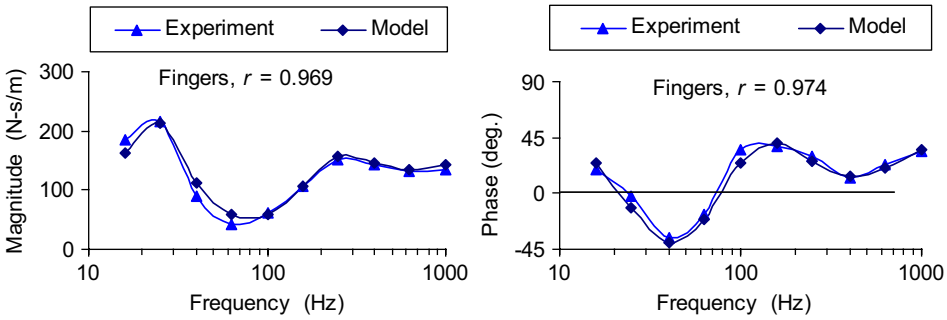

Fig. 6. Comparisons of model results with the experimental data in terms of mechanical impedance distributed at the fingers for the 50 N pull-only action.

Table 2
Parameters for the 5-DOF model

Parameter	Unit	Hand coupling condition (50 N applied in each action)			
		Grip	Grip + push	Push	Pull
M_0	Kg	5.0516	6.0887	2.5941	1.7008
M_1	Kg	1.4295	1.4197	0.9125	0.8435
M_2	Kg	0.0887	0.0818	0.3416	0.0982
M_3	Kg	0.0229	0.0266	0.0247	0
M_4	Kg	0.0150	0.0140	0	0.0137
K_0	N/m	149,490	9425	17,713	7226
K_1	N/m	1726	5382	834	3512
K_2	N/m	12,075	6347	1583	24,107
K_3	N/m	29,898	57,535	46,279	0
K_4	N/m	195,665	208,489	1763	167,117
C_0	N/m	87.2	97.5	1.2	2.1
C_1	N s/m	64.9	77.0	91.66	57.7
C_2	N s/m	36.3	38.0	0.4	37.3
C_3	N s/m	74.8	118.4	95.1	0
C_4	N s/m	126.0	120.6	4.7	110.8
$^*f_0$	Hz	27	8	13	13
$^*f_1$	Hz	28	35	16	30
$^*f_2$	Hz	245	258	37	222

$^*f_0$, f_1 and f_2 are the undamped natural frequencies of the model.

the f_2 values in Tables 1 and 2. This demonstrates that the finger resonance depends primarily on the effective mass of the fingers and their contact stiffness. On the hand, the palm resonance depends mainly on the effective mass of the palm–wrist–forearm structure and the palm contact stiffness, since the estimated frequency $\sqrt{k_3/M_1}$ is close to f_1 (grip: 23 Hz; grip + push: 32 Hz; and push: 31 Hz). Obviously, these resonances are associated with two different substructures of the hand gripping the handle. It is impossible to use the single-point coupling model to simulate such responses, which partially explains why the reported models cannot be generally interpreted in term of the anthropometry of the hand–arm system.

The parameters of the proposed models can be generally related to the applied hand forces and actions, and hand anthropometry. For examples, the values of M_4, M_2, k_4, and c_4 vary within relatively small bands in both models, irrespective of the hand actions (grip, grip + push, and pull), which is attributable to the identical fingers-applied force of 50 N. Owing to the nonlinear behaviors of soft tissues (Chaffin et al., 1999; Wu et al., 2006), an increase in the palm force from 50 N (grip only) to 100 N (grip and push) yield higher palm contact stiffness k_3. The effective mass due to palm skin M_3 is larger than that due to fingers' skin M_4, which is attributed to the higher contact area on the palm side (Aldien et al., 2005; Welcome et al., 2004). The effective fingers mass $M_2 + M_4$ is less than that estimated from the volume ($\approx$137 ml) (Dong et al., 2005b) and density ($\approx$1.16 g/ml) (Gibson and Ashby, 1997). This is also applicable to $M_1 + M_3$, which is less than that (1.67 kg) estimated from the hand–forearm volume (1828 ml) (Dong et al., 2005a). Moreover, the palm and finger resonance frequencies are similar to those observed in the vibration transmissibility values measured at the wrist and on the fingers, respectively (Kihlberg, 1995; Reynolds, 1977; Thomas and Beauchamp, 1998). These observations suggest that the fundamental dynamic characteristics of the hand–arm system with the hand coupled on the handle are reasonably represented by the proposed models.

Mass M_0 in the 5-DOF model can be excited only at low frequencies (<25 Hz) (Reynolds, 1977) but the experimental data used in this study are above 16 Hz. This explains why M_0 could take quite different values, as shown in Table 2. Its uncertainty could also affect the parameters of the elements connected to M_0. Further experimental studies under lower excitation frequencies are thus desirable to examine the validity of these parameters.

Only a few reported DPBR models have shown such good agreements between modeling predictions and experimental data as those observed in this study (Gurram et al., 1995; Rakheja et al., 2002). While the reported low-order models have shown relatively poor agreements with the experimental data, the high-order models generally yield excessive static deflections attributed to their low stiffness parameters (Rakheja et al., 2002). For example, the 3-DOF model described in ISO10068 (1998) yields a deflection of 9.37 mm between the hand and handle in the z_h-axis under a 50 N push force, which is considered to be unrealistic and would make it difficult to construct a hand–arm simulator. The proposed 4-DOF model is quite simple for fabrication of a hand–arm simulator, while the 5-DOF model can provide more information on the distributions of the biodynamic responses. For example,

Table 3
Comparisons of error rms values of the 4-DOF and 5-DOF models

Location	Impedance component	RMS values of model fitting error							
		Grip		Grip + push		Push		Pull	
		4-D	5-D	4-D	5-D	4-D	5-D	4-D	5-D
Fingers	Magnitude (N s/m)	7.96	7.18	7.17	7.12			11.29	9.43
	Phase (degree)	5.31	5.77	3.98	3.82			5.65	4.61
Palm	Magnitude (N s/m)	9.87	8.96	9.76	10.22	9.68	8.98		
	Phase (degree)	6.64	6.17	4.51	4.49	6.11	5.16		
Hand	Magnitude (N s/m)	12.11	11.51	15.87	16.03				
	Phase (degree)	5.75	5.64	3.07	3.03				

the damping value c_1 can be used to estimate the power absorption in the arm, which has been infeasible to be measured experimentally.

In conclusion, this study developed two models for simulating the distributed biodynamic responses of the hand–arm system exposed to vibration in z_h-axis. They can be used to further study the biodynamic responses and their applications.

Disclaimers

The content of this publication does not necessarily reflect the views or policies of the National Institute for Occupational Safety and Health (NIOSH), nor does mention of trade names, commercial products, or organizations imply endorsement by the US Government.

References

Aldien, Y., Welcome, D.W., Rakheja, S., Dong, R.G., Boileau, P.-E., 2005. Contact pressure distribution at hand–handle interface: role of hand forces and handle size. International Journal of Industrial Ergonomics 35, 267–286.

Chaffin, D.B., Andersson, G.B., Martin, B.J., 1999. Occupational Biomechanics. Wiley, New York.

Dong, R.G., Rakheja, S., Schopper, A.W., Han, B., Smutz, W.P., 2001. Hand-transmitted vibration and biodynamic response of the human hand–arm: a critical review. Critical Reviews™ in Biomedical Engineering 29, 391–441.

Dong, R.G., Wu, J.Z., McDowell, T.W., Welcome, D.E., Schopper, A.W., 2005a. Distribution of mechanical impedance at the fingers and the palm of human hand. Journal of Biomechanics 38, 1165–1175.

Dong, R.G., Wu, J.Z., Welcome, D.E., McDowell, T.W., 2005b. Estimation of vibration power absorption density in human fingers. Journal of Biomechanical Engineering 127, 849–856.

Gurram, R., Rakheja, S., Brammer, A.J., 1995. Driving-point mechanical impedance of the human hand–arm system: synthesis and model development. Journal of Sound and Vibration 180, 437–458.

Gibson, L.J., Ashby, M.F., 1997. Cellular Solids—Structure and Properties. University Press, Cambridge.

Griffin, M.J., 1994. Foundations of hand-transmitted vibration standards. Nagoya Journal of Medical Science 57(Suppl.), 147–164.

ISO8727, 1997. Mechanical Vibration and Shock—Human Exposure—Biodynamic Coordinate Systems. International Organization for Standardization, Geneva, Switzerland.

ISO 10819, 1996. Mechanical Vibration and Shock—Hand–Arm Vibration—Method for the Measurement and Evaluation of the Vibration Transmissibility of Gloves at the Palm of the Hand. International Organization for Standardization, Geneva, Switzerland.

ISO10068, 1998. Mechanical Vibration and Shock—Free, Mechanical Impedance of the Human Hand–Arm system at the Driving Point. International Organization for Standardization, Geneva, Switzerland.

Kihlberg, S., 1995. Biodynamic response of the hand–arm system to vibration from an impact hammer and a grinder. International Journal of Industrial Ergonomics 16, 1–8.

Rakheja, S., Wu, J.Z., Dong, R.G., Schopper, A.W., 2002. A comparison of biodynamic models of the human hand–arm system for applications to hand-held power tools. Journal of Sound and Vibration 249, 55–82.

Reynolds, D.D., 1977. Hand–arm vibration: a review of 3 years research. In: Proceedings of the Second International Conference on Hand–Arm Vibration, Cincinnati, OH, USA, pp. 99–128.

Thomas, M., Beauchamp, Y., 1998. Development of a new frequency weighting filter for the assessment of grinder exposure to wrist transmitted vibration. Computers and Industrial Engineering 35, 651–654.

Welcome, D.E., Rakheja, S., Dong, R.G., Wu, J.Z., Schopper, A.W., 2004. Relationship between the grip, push and contact forces between the hand and a tool handle. International Journal of Industrial Ergonomics 34, 507–518.

Wu, J.Z., Cutlip, R.G., Andrew, M.E., Dong, R.G., 2006. Simultaneous determination of the nonlinear-elastic properties of skin and subcutaneous tissue in unconfined compression tests. Skin Research and Technology 12, 1–9.